



# Transport of ozone towards the Alps – results from trajectory analyses and photochemical model studies

G. Wotawa<sup>a,\*</sup>, H. Kröger<sup>a</sup>, A. Stohl<sup>b</sup>

<sup>a</sup>Universität für Bodenkultur Wien, Institute for Meteorology and Physics (IMP), Türkenschanzstraße 18, A-1180 Vienna, Austria

<sup>b</sup>Technische Universität München, Lehrstuhl für Bioklimatologie und Immissionsforschung,  
Am Hochanger 13, D-85354 Freising-Weihenstephan, Germany

Received 25 January 1999; accepted 28 July 1999

## Abstract

We present results of statistical trajectory source analyses applied on ozone concentrations measured at high mountain peaks within and at the fringes of the Alps supported by Lagrangian photochemical box model calculations. These analyses yielded coherent pictures of transport processes causing elevated ozone concentrations in the Alps, and of the amount of ozone produced during transport over high-emission areas. Using measurement data, specific emission areas like the Po Basin, southern Germany, the “Black Triangle” region and some areas in eastern Europe were identified as important source regions, causing elevated ozone concentrations in the Alps. These statistics were supported by model calculations of transport and formation of ozone, giving similar results. Mesoscale transport processes and ozone formation in the boundary layer along the pathways were found to play an important role in determining Alpine ozone concentration levels. Ozone concentration tendencies along transport pathways were quantified climatologically using the box model. During the last 24 h of transport, concentration increases of 6–13 ppb, on the average, were found along 60–80% of all trajectories reaching the Alps, depending on the specific location. These estimates were confirmed by a measurement-based analysis of ozone formation during transport over the Po Basin, obtaining values of similar order of magnitude. © 2000 Elsevier Science Ltd. All rights reserved.

**Keywords:** Trajectories; Lagrangian transport; Box models; Ozone; Photochemistry

## 1. Introduction and basic objectives

Ozone (O<sub>3</sub>) concentrations in the Alps increased by a factor of two since 1950 (Staehelin et al., 1994). Free tropospheric O<sub>3</sub> concentrations, that influence high-Alpine mountain peaks, exhibited a far more pronounced upward trend than boundary layer concentrations (Wege and Vandersee, 1991). High O<sub>3</sub> concentrations can be caused by different processes, namely by downward transport of ozone-rich air from the stratosphere, by horizontal advection of ozone produced in polluted regions, or by in-situ formation due to local emissions. During the EU research project VOTALP (Wotawa and Kromp-Kolb, 2000) it was attempted to give estimates of

the relative importance of these processes compared with each other. In this paper, we focus on horizontal transport of O<sub>3</sub> from surrounding areas towards the Alps, but issues of vertical transport are also addressed. The study is based on the following questions to be answered in a statistical-climatological way:

- Which transport pathways are frequently associated with high O<sub>3</sub> concentrations observed in the Alpine region?
- Where is the O<sub>3</sub>, observed in the Alps, produced?
- How much O<sub>3</sub> may be formed during the last few days of transport towards the Alps?

To provide answers to these questions on the meso-β scale (10 × 10 km–100 × 100 km), we use background measurement data, calculated air-mass trajectories and Lagrangian photochemical box model results.

\* Corresponding author. Fax: + 43-1-470-58-2060.

E-mail address: gerhard.Wotawa@boku.ac.at (G. Wotawa)

The representativity of ground-level measurements of reactive trace gases is frequently affected by local influences. For instance, Tilmes and Zimmermann (1998) analysed  $O_3$  data from more than 300 German stations and found that the average radius of representativity was only about 3–4 km. This strongly limits the use of ground-level data to determine source regions of  $O_3$  on a larger scale. Mountain peak stations, as used in our study, are far more appropriate to study tropospheric background conditions. The average radius of representativity should be in the order of 100 km (as assumed, e.g. by the European Topic Center for Air Quality). But, to a certain extent, local influence can be imposed by thermally driven circulation systems (Vergeiner and Dreiseitl, 1987). During daytime, polluted air masses might be transported upwards to peak level by up-slope winds. To avoid any possible contamination, analyses presented here are to a large extent based on nighttime measurements, where down-slope flow predominates.

Our approach is to investigate horizontal transport processes by combining representative  $O_3$  measurement data from mountain peak stations located within and around the Alps with backward trajectories ending at these sites. Results of photochemical box model calculations are included in the discussion.

After an overview on methods applied and models used (Section 2), results of the investigations are presented (Section 3). We show and discuss results of three-dimensional trajectory statistics for high Alpine peak stations, allowing to differentiate between boundary layer  $O_3$  formation and advection from the middle or upper troposphere. Then, we focus on boundary layer  $O_3$  formation and discuss results of two-dimensional boundary layer trajectory statistics and of photochemical box model calculations. We identify emission regions important for increased  $O_3$  levels in the Alps and quantify the concentration increase of  $O_3$  along the transport pathways caused by these emissions. At last, we concentrate on the impact of a specific emission area, the Po Basin in northern Italy, and estimate the measured concentration increase of  $O_3$  during transport across this region. In Section 4, we provide a summary and draw conclusions.

## 2. Description and discussion of methods and models applied

For the purposes of this study, representative measurements from different mountain peak stations within

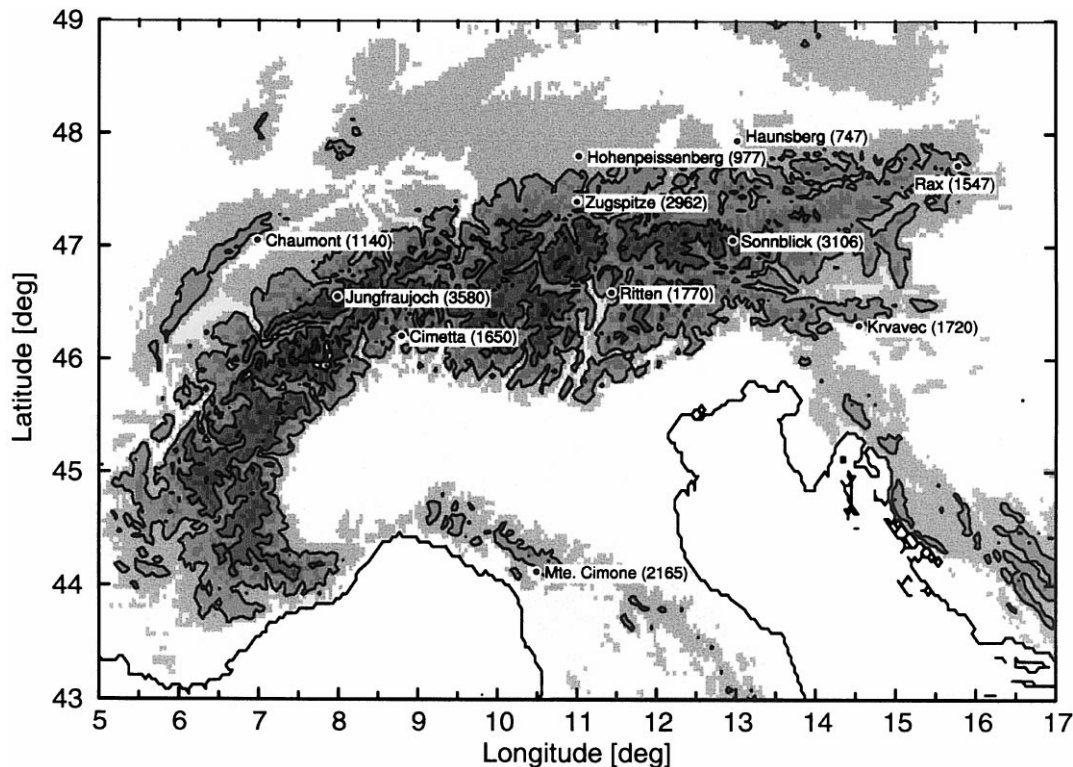


Fig. 1. Locations of ozone monitoring sites within and around the Alps used for the investigation of horizontal transport of  $O_3$  towards the Alpine region. The numbers in brackets denote the respective station height (m asl). Countour levels are spaced in 1000 m steps, gray scales in 500 m steps.

and around the Alps and Apennines are used. A map of the investigation area showing all locations is presented in Fig. 1. All sites are part of routine monitoring networks.

Applying the trajectory model FLEXTRA (Stohl et al., 1995) based on model-level wind fields from the global weather prediction model of the European Centre for Medium-Range Weather Forecasts, (ECMWF, 1995) available on a  $1^\circ \times 1^\circ$  geographical grid covering Europe and the Atlantic Ocean, backward air trajectories were calculated for the stations. Compared with the output of a free-running meteorological model, ECMWF analyses are preferable, because they remain fully consistent with observed meteorology at any time. The coarse spatial resolution of the ECMWF analyses corresponds with the scale of this investigation. Thermally driven circulation systems and other terrain-induced effects are only resolved on that scale, and thus smaller scale motions introduce noise into the results. The noise is potentially largest during daytime convective situations.

Two different sets of trajectories were calculated, namely three-dimensional (3-D) trajectories and two-dimensional (2-D) atmospheric boundary layer (ABL) trajectories. For the calculation of 3-D trajectories, we used the vertical wind velocity component  $d\eta/dt$  on ECMWF model levels, with  $\eta$  being the vertical coordinate of the model. The algorithm for computing boundary layer averaged trajectories was described by Stohl and Wotawa (1995). Both trajectory types show advantages and disadvantages. 3-D trajectories completely represent the 3-D nature of transport as long as turbulence does not destroy the identity of an air parcel. 2-D ABL trajectories best represent boundary layer transport, as demonstrated, e.g. by Haagensohn et al. (1990), since they partly consider the mixing in the ABL. For a comprehensive discussion of trajectory types, we refer to Stohl (1998).

Methods of trajectory statistics, as also discussed by Stohl (1998), have been developed to establish source-receptor relationships of pollutants, which are directly emitted and do not undergo non-linear chemical reactions. The application to secondary pollutants is not straight-forward, since the applicability can be restricted by non-linear chemical reactions and by resulting variable lifetimes of the transported species. In the case of  $O_3$ , short lifetimes and high non-linearity of chemistry predominate within urban plumes. But, besides the urban plumes, which only make up a relatively small percentage of the whole area, lifetimes increase significantly from hours to days, reaching months in the upper free troposphere. Taking this into account, one can say that, although  $O_3$  is no perfect tracer, it is a usable tracer for the purposes of trajectory statistics on the time scale considered. Trajectory-based statistical methods have already been successfully applied to  $O_3$  measurements in the past (see, e.g. Stohl and Kromp-Kolb, 1994; Sirois

and Bottenheim, 1995; Wotawa, 1997; Brankov et al., 1998).

Taking into account that transport, especially in complex terrain, is a 3-D process and that high mountain sites are located within the free troposphere during most of the time, we first applied a 3-D trajectory statistics based on 3-D trajectories on  $O_3$  measurement data from high Alpine mountain peak observatories to study typical transport patterns. Afterwards, we focused on long-range boundary-layer  $O_3$  transport processes towards the Alps. For that purpose, we applied a 2-D trajectory statistics on  $O_3$  measurement data, based on ABL trajectories. For this investigation, we selected different measurement locations at lower altitudes on peaks or slopes at the fringes of the Alpine region or a short distance away (Alpine foothills, Pre-Alps and Jura), where we assumed that horizontal transport processes can be better described by ABL trajectories.

3-D trajectory statistics were calculated combining 3-D trajectories with three-hourly averaged  $O_3$  concentrations at the high-Alpine peak observatories Jungfraujoch, Sonnblick and Zugspitze, and at Mte. Cimone, the highest peak in the northern Apennines. Applying the concentration field method after Seibert et al. (1994), a grid with a resolution of  $1^\circ \times 1^\circ$  is superimposed on the computational domain, and the  $O_3$  concentration measured at the receptor location is attributed to all grid cells crossed by the appropriate trajectory. From all realizations, average concentration fields are calculated. A high concentration value in a grid cell means that, on the average, air parcels crossing over this cell result in high concentrations at the receptor location. Similar studies of sulphur components reaching Mount Sonnblick were performed by Tschirwenka et al. (1998) and Seibert et al. (1998). They showed that 3-D trajectories realistically simulate the transport of polluted boundary layer air up to this mountain site. An important problem for the representation of transport pathways to mountain sites using trajectories is that the model topography and the real topography differ considerably. For this reason, it is not trivial at what height the back trajectories shall terminate. For instance, they may end at the height of the model topography, or at the corresponding height above sea level of the station. In our case, since we are mostly interested in the large-scale flows, we chose the latter possibility, since the lowermost ECMWF model levels are influenced by the artificial absence or presence of local slope flows, due to differences between model and real topography.

For the investigation of the importance of boundary layer  $O_3$  formation and transport towards the Alps, we use ABL trajectories computed for the background stations Chaumont, Cimetta, Ritten, Krvavec, Rax, Haunsberg and Hohenpeißenberg. Wotawa and Kröger (2000) used the same setup (same trajectories, same locations) to validate trajectory statistics, successfully reproducing the

European inventory of nitrogen oxides emissions from model simulations of  $\text{NO}_y$  performed along the same trajectories. In this paper, we apply a similar 2-D statistics based on a residence time analysis as suggested by Ashbaugh et al. (1985). Relative residence time (RRT) is defined as residence time of trajectories within a grid cell given that a selected threshold concentration (in this study the 90th percentile value) of  $\text{O}_3$  is exceeded at the receptor location of the trajectory, divided by the total residence time of all trajectories within that grid cell. This can be interpreted as conditional probability. Trajectories crossing regions with high values of RRT and thus high conditional probability have a large potential to be associated with high  $\text{O}_3$  concentrations at the receptor sites. To identify regions potentially responsible for the highest 10% of the  $\text{O}_3$  concentrations in the Alps, RRT values were evaluated on a regular  $0.5^\circ \times 1^\circ$  grid.

To raise confidence in the study of regions influencing high  $\text{O}_3$  concentrations measured in the Alpine region, we performed photochemical box model simulations of ozone formation and transport along the ABL trajectories. For that purpose, we applied the IMPO Lagrangian photochemical box modelling system (Wotawa et al., 1998). The box side-lengths were increased from 50 km at the receptor locations to 225 km at 168 h backwards in time, assuming zero-gradient lateral boundary conditions.

A different method was applied to assess  $\text{O}_3$  production during transport across the Po Basin. Differences between up-stream and down-stream  $\text{O}_3$  concentrations were evaluated statistically.  $\text{O}_3$  concentrations south of the Po Basin were obtained from measurements at Mte. Cimone, whereas concentrations north of the Po Basin were taken from measurements at Jungfraujoch, Cimetta, Ritten and Krvavec. Three-dimensional trajectories were used for this analysis. North–south and south–north flows were evaluated separately. We only considered trajectories showing residence times of at least four hours above the high-emission areas of the Po Basin. During north–south flow, we followed the trajectory from Mte. Cimone backwards until the time of closest passage to one of the Alpine sites. Then, we subtracted the  $\text{O}_3$  concentration from this site at the time of closest passage from the concentration measured at Mte. Cimone at the time when the trajectory ended. All concentrations represent 3 h averages. In the case of south–north flow we used trajectories coming close to Mte. Cimone. We subtracted the concentration measured at Mte. Cimone at the time of closest passage from the concentration measured at the Alpine site during the ending time of the trajectory. We skipped trajectories if the distance of closest passage exceeded 300 km. This larger distance was selected to increase the number of trajectories included and thus the statistical significance. Since only background stations outside the Po Basin are used for this analysis, this radius is justifiable. To ensure maximum influence of polluted boundary-layer air, only cases where trajectories arrived

between 12 and 18 UTC were considered for subsequent statistical evaluation. This is a difference to our trajectory statistics, where we only used nighttime  $\text{O}_3$  measurements. Transport of polluted air masses from the Po Basin towards the sites with up-slope winds was, contrary to trajectory statistics, a wanted effect for this evaluation.

### 3. Results

#### 3.1. Results of 3-D trajectory statistics

For the statistical evaluation, 3-D trajectory data were available every 3 h between January 1995 and March 1998. For Sonnblick and Jungfraujoch, measurement data were available during the full period; for Zugspitze, data were available only from January 1995 to September 1997; and for Mte. Cimone, data were available only from March 1996 to October 1997. To eliminate unresolved local contamination by thermally driven up-slope winds (Vergeiner and Dreiseitl, 1987), we excluded afternoon data from 11:30 to 20:30 local time.

The statistics were calculated for different height intervals of the trajectories to account for the dependence on height of the source regions. We do not present the results for the four stations individually. Instead, we merged the whole dataset to achieve higher statistical significance and better spatial coverage. Furthermore, the different concentration levels at the four stations and their attribution to the trajectories provide additional information on source regions (Stohl, 1996). However, it was checked that the structures obtained with the combined dataset are consistent with the structures seen for the individual stations.

The ozone concentration field for the 0–2500 m height interval (see Fig. 2) is the one most influenced by regional  $\text{NO}_x$  and VOC sources. In the concentration fields at the upper levels (not shown here), there is far less structure. Note, however, that since the low-level trajectories had to ascend to arrive at the mountain summits, meteorological conditions along the ascending parts of the trajectories were not associated with meteorological conditions particularly conducive to photochemical ozone formation.

On the largest scale, the European continent appears as a source of  $\text{O}_3$ , the highest concentrations being located in eastern Europe. During the summer, the European continent was also found to be a net  $\text{O}_3$  source for the north Atlantic in a study of Derwent et al. (1998). Trajectories arriving from the east have to cross many emission sources and typically experience sunny weather, the combination of which may result in strong photochemical  $\text{O}_3$  formation. Similar results from trajectory statistics were also obtained for the Vienna region (Stohl and Kromp-Kolb, 1994). Two regions appear as local

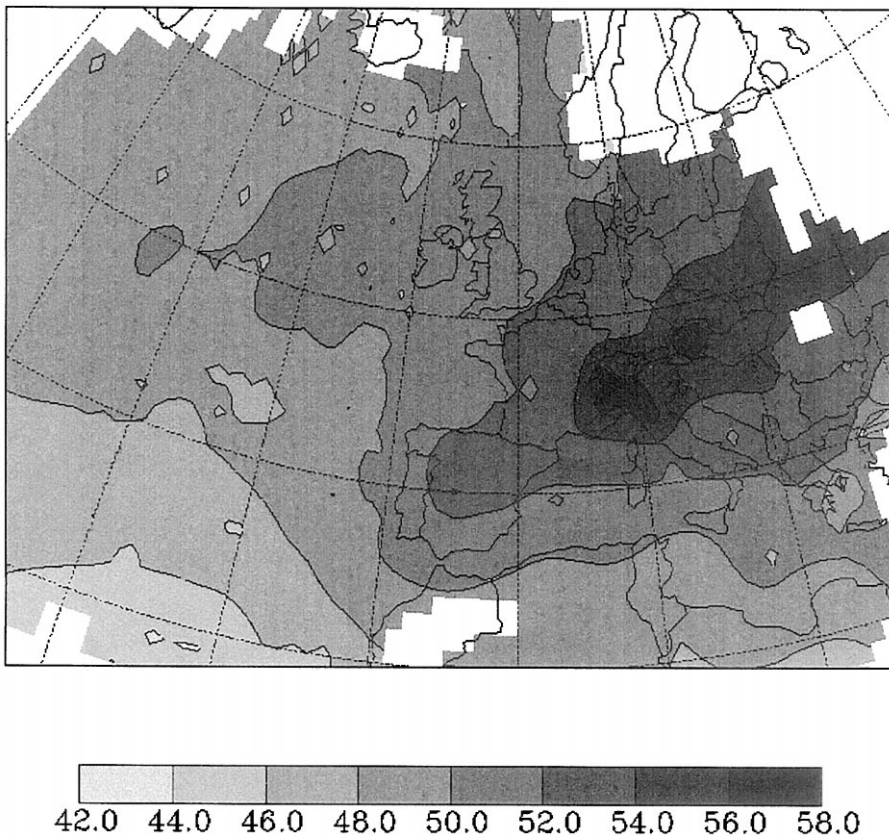


Fig. 2. Concentration fields of O<sub>3</sub> (ppb) obtained with trajectory statistics applied to ozone measurement data from Mte. Cimone (03/1996–10/1997), Zugspitze (01/1995–09/1997), Sonnblick and Jungfraujoch (01/1995–03/1998) and to trajectory positions below 2500 m. Data between 11:30 and 20:30 local time were excluded from the statistics. Grid cells that were crossed by less than 20 trajectories are left blank. The receptor locations are marked with asterisks.

maxima in the concentration fields: First, the Po Basin region, where emissions of primary pollutants are among the highest in Europe, and, second, eastern Austria. The Po Basin has already been identified to cause high O<sub>3</sub> concentrations in the Alps (e.g. Prevot et al. (1997)). For the trajectories travelling via eastern Austria the cumulative emissions of eastern Europe are probably important to generate a high background O<sub>3</sub> level. O<sub>3</sub> formation in the plumes of the cities of Bratislava, Vienna, Linz and Graz may then be responsible for producing the second local maximum. The Munich area north of the Alps does not seem to have a strong effect on the O<sub>3</sub> concentrations in this evaluation. This is probably due to the weather conditions being not so conducive for O<sub>3</sub> formation during transport from the north.

Low O<sub>3</sub> concentrations are found in air that comes from the Atlantic Ocean, with the lowest concentrations coming from the south. This north–south gradient may have two reasons: first, O<sub>3</sub> is rapidly destroyed by photolysis in the subtropical marine boundary layer; second,

injection of stratospheric air into the troposphere occurs mainly at the polar front (Parrish et al., 1998). Of course, trajectories reaching the Alps from the Atlantic have to cross emission areas as well. However, the results of the statistics for these areas are dominated by “slow” trajectories (concentrations are weighted with residence times!). Thus, the lower concentrations over the Atlantic are no artefact of the method, but represent reality. Virkkula et al., 1995, 1998) found a very strong ocean–continent gradient in several species applying a similar method, but for a site closer to the ocean. Similar gradients, however, were also found by Stohl (1996) and Wotawa and Kröger (2000) for receptor locations far away from the Atlantic.

At higher levels (the highest one used all trajectory points above 5000 m), the spatial gradients in the concentration fields are much weaker (not shown here). Especially, the Po Basin and eastern Austria disappear as O<sub>3</sub> sources, but a corridor of high concentrations connects the region around Iceland with the receptors. This corridor most likely indicates intrusions of stratospheric

air. This conclusion is supported by another, detailed study on stratospheric intrusions impinging on the Alps, where it could be shown that these events typically are associated with transport from the north-west (Stohl et al., 2000).

In the summer half-year, the major source regions are the same as those identified for the whole year, the major difference being a higher concentration level and somewhat stronger spatial gradients. In the winter half-year, the European continent appears as a much weaker source of  $O_3$ . In contrast to the summer half-year, descending trajectories bring higher concentrations than ascending trajectories, providing evidence for the existence of an upper tropospheric or stratospheric  $O_3$  source that is more important than regional photochemical  $O_3$  production during that time of the year.

### 3.2. Results of 2-D boundary layer trajectory statistics

Since the focus of these statistics is on photochemical  $O_3$  formation in the boundary layer due to regional emission sources, they are restricted to summer half-years. Calculated ABL trajectories and measurement data were available from April to September 1995 and 1996, respectively.

The stations Cimetta and Krvavec are situated at mountain peaks in the southern foothills of the Alps, Haunsberg and Hohenpeissenberg in the northern foothills. The Rax peak is situated in the Alps southwest of Vienna. The measurement station is located on a slope approximately 400 m below the summit. The station Ritten lies approximately 80 km north of the southern foothills within the Alps and is surrounded by higher peaks. The station Chaumont is situated on the southern slope of the Jura in western Switzerland. Mean measured  $O_3$  concentrations for the two summer half-years are about 45 ppb north of the Alps, 50 ppb west and east of the Alps and 55 ppb in the south.

The RRT analyses for the highest 10% of the measured  $O_3$  concentrations were first performed for all cases. Afterwards, the statistics were restricted to fair-weather cases, because the (partly even linear) relationship between  $O_3$  and  $NO_y$  concentrations (supporting the applicability of the statistics) as shown for rural locations (Sillman et al., 1990) is disturbed under weather conditions not conducive to  $O_3$  formation. A fair-weather situation was assumed if cloud cover averaged along a trajectory was less than or equal to 0.6.

Sensitivity studies showed that results did not change significantly if one station was excluded or if one station was replaced by another situated nearby. To avoid a possible influence of daytime up-slope winds on the results, the statistics was only applied to  $O_3$  concentrations measured at 2 UTC. The sensitivity of the results of the statistics to the selection of the trajectory type was tested, showing that results obtained with 3-D trajectories did

not deviate significantly from those obtained with the ABL trajectories (not shown here). Trajectories crossing the Alps were excluded from the evaluation, since cross-Alpine transport is not reproduced reasonably using ABL trajectories. To avoid unrealistic structures due to insufficient data coverage in certain grid cells, RRT values were calculated only if a minimum of 15 trajectories hit the respective cell.

The results of the 2-D statistics for all cases (Fig. 3, top, left picture) are in fair agreement with the results of the 3-D statistics. The Po Basin is identified again as an important source region, and high RRT values extend from the Alps towards the east. Southern Germany is again not identified as important source region. As a difference to the 3-D statistics, eastern Austria is also not identified. In previous studies (Stohl and Kromp-Kolb, 1994; Wotawa, 1997), it was shown that typical  $O_3$  episodes in eastern Austria occur during southeasterly flow conditions. The eastern Alpine receptor location, Rax, which is situated southwest of Vienna, is not directly influenced by the  $O_3$  plume of Vienna during such situations.

A restriction of the statistics to fair-weather conditions (Fig. 3, top, right picture) shows a slightly smaller influence of the eastern regions, but a clearly higher contribution of southern Germany and the so-called black triangle, a high emission area situated at the German-Polish-Czech border. Almost no high  $O_3$  values are transported from western and northwestern directions towards the Alps.

### 3.3. Results of photochemical box modelling

Without subsequent photochemical modelling, the results of the 2-D trajectory statistics are difficult to interpret in two respects: First, measured  $O_3$  concentrations may be influenced by subgrid-scale transport processes or by advection of high concentrations from the middle or upper troposphere. Such processes may be systematic and thus might lead to erroneous identifications of source areas. Second, the statistical method does not account for non-linear chemical reactions, again possibly leading to wrong identifications. To overcome these problems, a Lagrangian photochemical box model, the IMPO model, was applied to calculate pollutant concentrations along the ABL trajectories. Since the model integrates our current knowledge about boundary layer  $O_3$  formation, deposition and transport, it was of interest to see whether the RRT maxima calculated from the measurements can be explained by the model or not, and in which regions high photochemical  $O_3$  production rates predominate along trajectories reaching the Alps later on.

To avoid a large dependency of model results on the initial pollutant concentrations, each simulation was performed for seven days. The first four days can be

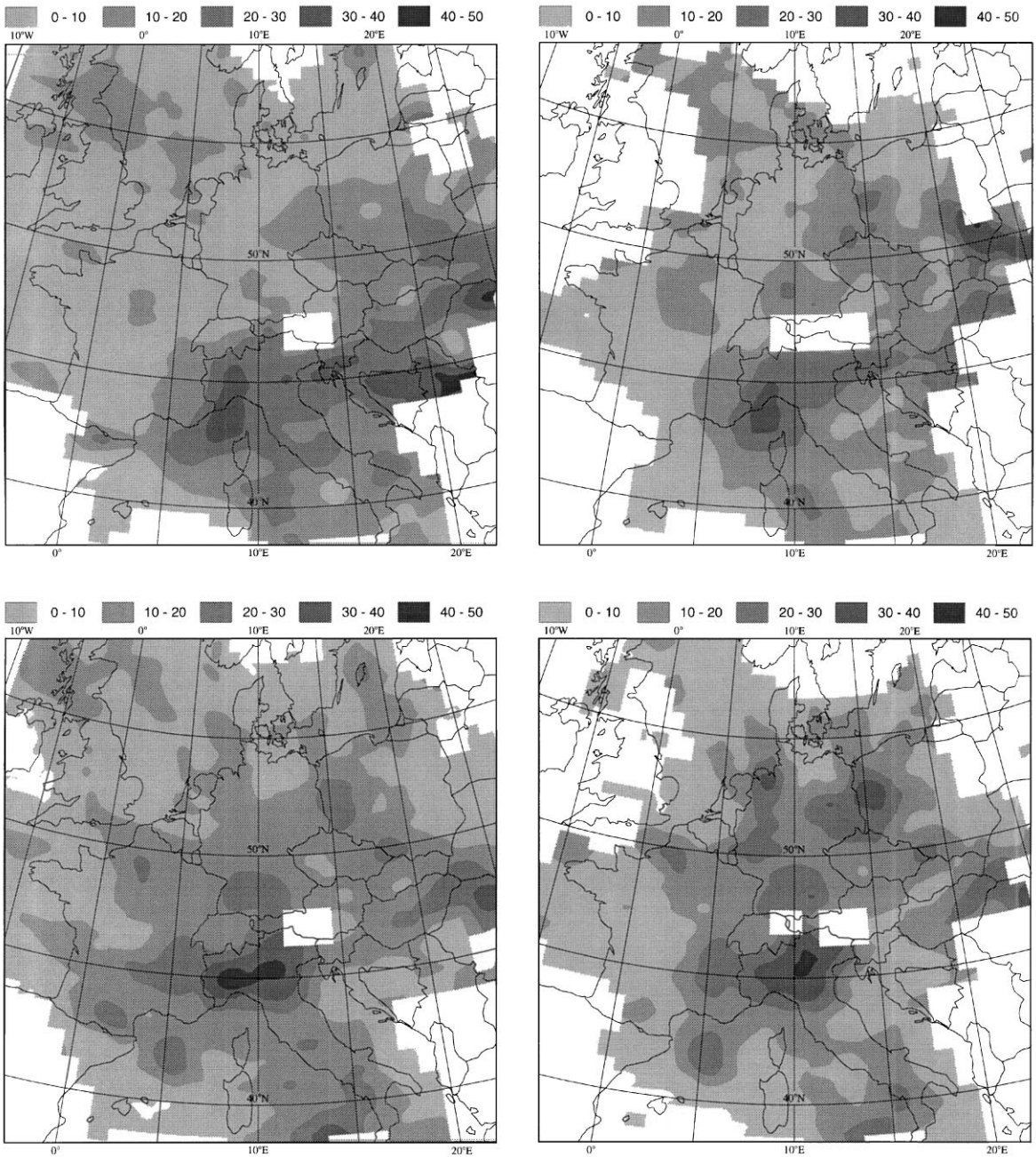


Fig. 3. Relative residence times (%) resulting from a 2-D boundary layer trajectory statistics calculated for the summer half-years (Apr.–Sept.) 1995–1996, based on measured (top) and modelled (bottom) nighttime (2 UTC) ozone concentrations at seven receptor locations. Modelled concentrations are taken from the fourth box (300–500 m agl) of a photochemical box model. The statistics were calculated for the whole sample (left) and for fair-weather cases only (right). For further explanation refer to the text.

considered as model spin-up period to provide realistic initial conditions for the last three days, which were used for further analysis. The results of photochemical modelling were used in three ways: First, we fed the calculated  $O_3$  concentrations into our trajectory statistics, to see

whether the results are consistent with those obtained with the measurement data. Second, calculated 1 h averaged photochemical net  $O_3$  production rates were statistically evaluated on a grid to identify regions where high production rates occur frequently. Third,

calculations were used to quantify how much  $O_3$  was formed along trajectories ending in the Alpine region during the last days of transport. These simulated values were compared with the observed ones for trajectories crossing the Po Basin (see Section 3.4).

Results of the 2-D trajectory statistics based on simulated  $O_3$  concentrations are shown in Fig. 3, bottom. A comparison of model-based statistics with measurement-based statistics confirms most of the identified source areas. Po Basin, southern Germany and the black triangle region are identified again as major source areas during fair-weather conditions. RRT maxima in the east and southeast are also reasonably reproduced by the model. The major disagreement between model-based and measurement-based statistics was found in northwestern parts of Europe (Belgium, the Netherlands and northwestern Germany) during fair-weather conditions. According to the model, highly-industrialized areas located there should have some influence on Alpine  $O_3$  concentrations, whereas no influence is seen in the measurement-based statistics.

The good consistency between model- and measurement-based statistics strongly supports our results, demonstrating that subgrid-scale transport as well as vertical transport processes of  $O_3$  towards the sites, which are not included in the modelled, but influence the measured  $O_3$  concentrations, did not degrade the results too much.

It does not mean, however, that vertical transport processes are not relevant. Especially during spring and autumn, it was shown in other studies that stratosphere–troposphere exchange is very important for Alpine  $O_3$  concentrations

Further on, the geographical distribution of high simulated photochemical net  $O_3$  production rates (1 h averages) was studied along trajectories reaching the Alps. Unlike the trajectory statistics, this shows in which regions chemical  $O_3$  production in the model takes place. To be consistent with the trajectory statistics, we considered only trajectories arriving at 2 UTC. To avoid a systematic reduction of high rates with increasing distance from the receptor locations due to the assumed increase of parcel diameters (see Section 2), these analyses are based on additional model runs where the parcel diameter was kept constant (50 km). The statistical analyses were done on the same grid as the trajectory statistics. First, we calculated the average of all positive  $O_3$  production rates within the grid cells (Fig. 4, left), if at least five positive rates did exist. Second, we calculated the percentage of occurrence of production rates larger than  $2 \text{ ppb h}^{-1}$  within the same sample (Fig. 4, right).  $2 \text{ ppb h}^{-1}$  is twice the average for the whole grid.

The highest average production rates and the highest frequency of increased rates were found for the Po Basin, large parts of Italy, southern Germany, parts of eastern

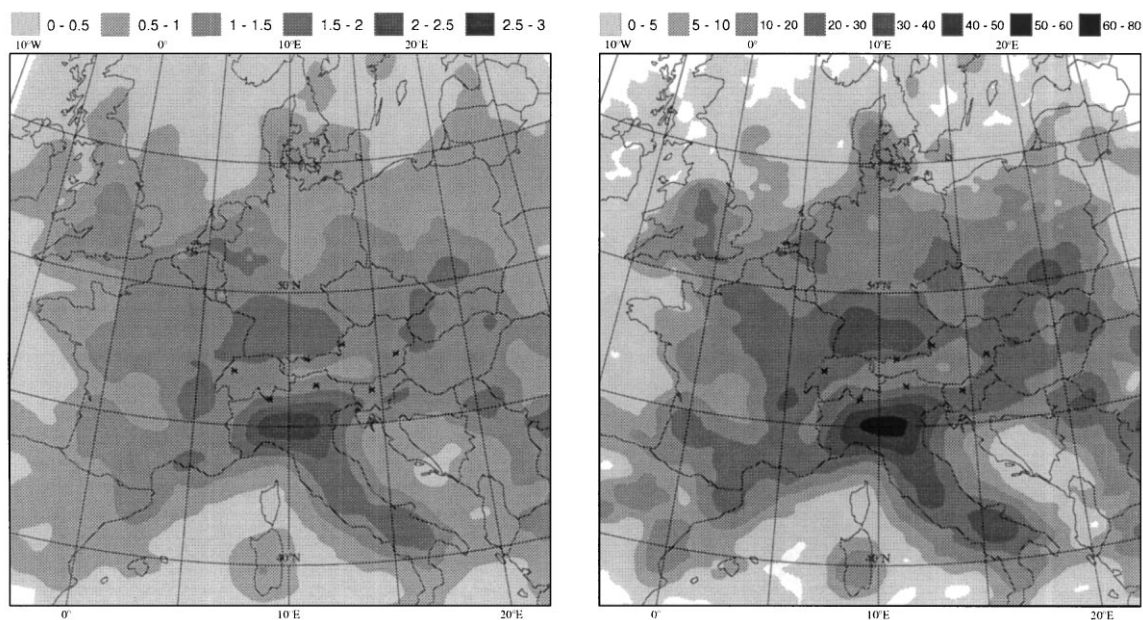


Fig. 4. Chemical  $O_3$  production rates calculated with a photochemical box model (third box: 100–300 m agl) along all trajectories reaching the Alpine region at 2 UTC during the summer half-years 1995 and 1996. The left picture shows the average of all positive  $O_3$  production rates ( $\text{ppb h}^{-1}$ ) within each grid cell, the right the percentage of occurrence (%) of  $O_3$  production rates that exceed  $2 \text{ ppb h}^{-1}$  within the same sample of data. Grid cells with less than five positive production rates are left blank. The production rates as presented here represent net budgets from chemistry, averaged over 1 h.

France, eastern Austria, parts of the Czech Republic, Hungary, Slovakia and Poland. Some spots with high O<sub>3</sub> production rates also exist in southeastern Europe. The high frequency of above-average O<sub>3</sub> production rates in central parts of Europe is certainly not only due to the emissions there, but O<sub>3</sub> formation is also triggered by the background pollution level, which is built up during several days of transport across European emission areas, especially if fair-weather conditions prevail along transport pathways.

The temporal development of the simulated afternoon O<sub>3</sub> concentrations along the trajectories approaching the Alpine region was studied climatologically for the two summer half-years. An increase of afternoon concentrations during the last 24 h of transport was found in 63–92% of the cases, depending on the receptor location. Highest average O<sub>3</sub> increases during the last 24 h were found for the southern locations Ritten (13 ppb) and Cimetta (9 ppb), lowest for the eastern and southeastern sites Rax (6.5 ppb) and Kravec (5.5 ppb). Maximum O<sub>3</sub> increases during 24 h of up to 40 ppb were calculated south of the Alps, up to 30 ppb for all other locations.

### 3.4. Influence of the Po Basin

Since the Po Basin was identified as the most important single source region for O<sub>3</sub> precursors in all our analyses, and since this is also known from previous (Prevot et al., 1997) or recent (Seibert et al., 2000) studies, we estimated O<sub>3</sub> formation along trajectories crossing the Po Basin using measurements in the Alps and Apennines and 3-D backward trajectories (see Section 2). The investigation period comprises the summer half-year 1996.

To get a first impression of the potential impact of O<sub>3</sub> formation in the Po Basin, an O<sub>3</sub> episode occurring on June 13, 1996 was studied in detail. On that day, an O<sub>3</sub> concentration of 117 ppb was recorded at Mte. Cimone. This belongs to the highest concentration values measured there during the whole year. The corresponding 3-D backward trajectory revealed that the air was transported across the Po Basin, with more than 15 h residence time above the high-emission areas. After crossing the Alps from the north, the trajectory propagated down to the Po Basin and subsequently ascended to the peak of Mte. Cimone, indicating an influence of boundary layer air. O<sub>3</sub> concentrations in the southern Alps at the time of trajectory passage amounted to 53 ppb on the average with a maximum of 60 ppb. Therefore, a total of 60 ppb additional O<sub>3</sub> seems to have been produced due to the emissions in the Po Basin.

A trajectory-based statistical evaluation of the O<sub>3</sub> excess concentrations on the downstream side of the Po Basin (see Table 1) yielded the following results: During north–south flow conditions, a positive excess O<sub>3</sub> concentration was observed downstream in 72% of the cases,

Table 1

Results of a statistical evaluation of the excess O<sub>3</sub> concentrations for transport over the Po Basin

	<i>N</i>	%	UsC (ppb)	DsC (ppb)	Excess (ppb)
NS <sub>1</sub>	122	100	55.6	62.3	6.7 (3.7--9.8)
NS <sub>2</sub>	108	89	55.9	63.1	7.2 (4.0--10.5)
NS <sub>3</sub>	88	72	53.2	64.1	10.9 (7.1--14.8)
SN <sub>1</sub>	157	100	58.0	63.6	5.6 (2.2--9.0)
SN <sub>2</sub>	76	48	60.1	72.4	12.3 (7.1--17.5)
SN <sub>3</sub>	89	57	57.9	72.7	14.8 (10.4--19.0)

“NS” denotes flow from north to south, “SN” the opposite direction. The subscript “1” denotes all cases, “2” cases with fair-weather conditions (cloud-cover less than 0.3 along trajectories crossing the Po Basin), and “3” cases with downstream concentrations > upstream concentrations. “UsC” are the mean upstream O<sub>3</sub> concentrations, “DsC” the mean downstream O<sub>3</sub> concentrations and “Excess” is the mean difference between downstream and upstream O<sub>3</sub> concentrations [ppb]. In brackets, the upper and lower confidence limits (98% confidence level) for the mean excess concentrations are specified. In total, 549 cases were investigated from 1 April to 30 September, 1996.

the average excess amounted to 11 ppb. In 89% of the cases, fair-weather conditions predominated in the Po Basin. Fair-weather conditions were assumed if the cloud cover in the Po Basin, averaged between beginning and ending time of trajectory passage, was less than 0.3. South–north flow conditions occurred somewhat more frequent. Only 48% were associated with fair-weather conditions. Consequently, only 57% of the cases exhibited excess O<sub>3</sub> concentrations, which amounted to 12 ppb on the average. Taking into account all cases, the excess concentrations amounted to 6 ppb. Depending on weather and air-chemical conditions, the Po Basin may act as source or sink of ozone. The source function, however, seems to predominate.

Summing up, we found a statistically significant (98% confidence level) O<sub>3</sub> increasing effect of the Po Basin at Alpine and Apenninian peak stations during all weather and flow conditions. This effect can amount up to some tens of ppb in single cases. Typical values are 6 ppb on the average and 7–12 ppb during fair weather conditions. The south foehn case investigated during VOTALP (Seibert et al., 2000) fits well into this general picture. O<sub>3</sub> concentrations at the Nordkette above Innsbruck, Tyrol, were elevated compared to Mte. Cimone by 10 ppb during some hours after the onset of foehn flow.

At last, a more or less qualitative comparison was done between measured O<sub>3</sub> increases along trajectories crossing the Po Basin and modelled concentration increases along trajectories reaching the south-Alpine sites of Cimetta and Ritten (to a large extent also Po Basin crossing trajectories, since cross-Alpine trajectories were excluded). Measurements indicate that

cross-Po Basin trajectories coming from the south show O<sub>3</sub> increases in 60% of all cases with an average excess of 15 ppb. Model results, depending on the location south of the Alps, show increases in 65–90% of all cases with averaged excess concentrations of 8–12 ppb. Maxima in the measurements show increases of 60 ppb, while maximum modelled excess concentrations are 40 ppb. This is, at least in a qualitative way, a good correspondence, indicating that model simulations of O<sub>3</sub> production along the trajectories are reliable on that scale.

#### 4. Summary and Conclusions

Analyses of O<sub>3</sub> measurements at mountain peak stations within and around the Alps together with calculated 3-D and ABL backward trajectories and photochemical box model simulations yielded coherent pictures of the transport processes causing elevated O<sub>3</sub> concentrations, and of the amount of O<sub>3</sub> produced during transport over high-emission areas like the Po Basin.

Boundary layer O<sub>3</sub> formation caused by European emissions was found to be very relevant for the Alps climatologically as well as in single cases during summer time. Important emission regions influencing Alpine O<sub>3</sub> concentrations were identified, namely the Po Basin, southern Germany, the black triangle region and eastern Europe as a whole. The latter, rather diffuse source area was identified probably due to a combination of high emissions and a preference for fair-weather conditions. On the other hand, for major emission areas in northwestern Europe, for instance the Ruhr area, no direct influence on Alpine O<sub>3</sub> concentrations was found. This may be due to weather conditions being frequently not favourable for O<sub>3</sub> formation during northwesterly advection.

During the winter, high O<sub>3</sub> concentrations are observed for air masses descending from the middle or upper troposphere. During the summer season, boundary layer O<sub>3</sub> formation is the dominant process. But, the clear separation between horizontal transport on one hand and vertical transport on the other is difficult. Especially combined effects – photochemical O<sub>3</sub> formation triggered by O<sub>3</sub> transported downwards from the higher troposphere or lower stratosphere – deserve further research activities. Anyway, it could be shown here that export of polluted boundary layer air from high-emission areas in Europe significantly affects O<sub>3</sub> concentrations in the free troposphere over Europe.

A better understanding has been achieved of the relative importance of several processes leading to high O<sub>3</sub> concentrations at Alpine peak level. Model studies indicate that advection of polluted air masses towards the Alps and the subsequent O<sub>3</sub> formation along the pathways leads to a net O<sub>3</sub> gain of 6–13 ppb during

the last day of transport, with the maximum at the southern side of the Alps. Using measurement data, an effect of the Po Basin was found in 57–72% of the cases, yielding averaged excess concentrations of 11–15 ppb. These numbers obtained for a specific emission region strongly support the model predictions. In cases of direct influence from urban plumes, O<sub>3</sub> concentrations at mountain peak level can increase by 50–60 ppb during some hours of transport.

High simulated photochemical net O<sub>3</sub> production rates were frequently found in central parts of Europe. This cannot only be explained by the emissions in some areas like the Po Basin, the Swiss Plateau, southern Germany and eastern Austria, but also with the high background pollution level that was built up during some days of transport over the European continent. Both, the emissions from nearby areas and the European emissions as a whole have to be considered for developing effective O<sub>3</sub> reduction strategies for the Alps.

#### Acknowledgements

This study was part of the research project “Vertical ozone transports in the Alps” (VOTALP). VOTALP was funded by the European Commission under Framework Programme IV, Environment and Climate, Contract number ENV4-CT95-0025, and by the governments of Switzerland and Austria. Meteorological model data were provided by ECMWF, Reading, UK. Meteorological measurement data were provided by the Central Institute of Meteorology and Geodynamics, Austria. Ambient air quality data were contributed by the Austrian Environmental Protection Agency, by the Office for Environmental Protection of the Austrian Federal State Salzburg, by the German Weather Service, by the Swiss Federal Office of Environment, Forests and Landscape, by the Office for Environmental Protection of the Swiss Canton Ticino, by the Office for Environmental Protection of the Italian province of South Tyrol and by the Hydrometeorological Institute of Slovenia. We would like to express thanks to all these organisations and their representatives. Furthermore, thanks are due to Dr. Bonasoni, CNR-ISA0, Bologna, for providing data from Mte. Cimone, to Dr. Scheel, Fraunhofer Institute for Atmospheric Environmental Research, Garmisch, for providing Zugspitze data, and to Dr. Gomisek for his help to get data from Krvavec, Slovenia.

#### References

- Ashbaugh, L.L., Malm, W.C., Sadeh, W.Z., 1985. A residence time probability analysis of sulfur concentrations at Grand Canyon National Park. *Atmospheric Environment* 19, 1263–1270.

- Brankov, E., Rao, S.T., Porter, P.S., 1998. A trajectory-clustering-correlation methodology for examining the long-range transport of air pollutants. *Atmospheric Environment* 32, 1525–1534.
- Derwent, R.G., Simmonds, P.G., Seuring, S., Dimmer, C., 1998. Observation and interpretation of the seasonal cycles in the surface concentrations of ozone and carbon monoxide at Mace Head, Ireland, from 1990 to 1994. *Atmospheric Environment* 32, 145–157.
- European Centre for Medium Range Weather Forecasts, ECMWF, 1995. User Guide to ECMWF Products Version 2.1. ECMWF, Reading, UK, 71 pp.
- Haagenson, P.L., Gao, K., Kuo, Y.H., 1990. Evaluation of meteorological analyses, simulations and long-range transport calculations using ANATEX surface tracer data. *Journal of Applied Meteorology* 29, 1268–1283.
- Parrish, D.D., Trainer, M., Holloway, J.S., Yee, J.E., Warshawsky, M.S., Fehsenfeld, F.C., Forbes, G.L., Moody, J.L., 1998. Relationships between ozone and carbon monoxide at surface sites in the North Atlantic region. *Journal of Geophysical Research* 103, 13357–13376.
- Prevot, A.S.H., Staehelin, J., Kok, G.L., Schillawski, R.D., Neining, B., Staffelbach, T., Nefel, A., Wernli, H., Domen, J., 1997. The Milan photooxidant plume. *Journal of Geophysical Research* 102, 23375–23388.
- Seibert, P., Kromp-Kolb, H., Baltensberger, U., Jost, D.T., Schwikowski, M., 1994. Trajectory analysis of high-alpine air pollution data. In: Gryning, S.-E., Millan, M.M. (Eds.), *Air Pollution Modelling and its Application X*. Plenum Press, New York, pp. 595–596.
- Seibert, P., Kromp-Kolb, H., Kasper, A., Kalina, M., Puxbaum, H., Jost, D.T., Schwikowski, M., 1998. Transport of polluted boundary layer air from the Po Valley to high-Alpine sites. *Atmospheric Environment* 32, 4075–4085.
- Seibert, P., Feldmann, H., Neining, B., Baumle, M., Trickl, T., 2000. South Foehn and Ozone in the Eastern Alps – case study and climatology. *Atmospheric Environment* (special VOTALP section), submitted for publication.
- Sillman, S., Logan, J.A., Wofsy, S.C., 1990. The sensitivity of ozone to nitrogen oxides and hydrocarbons in regional ozone episodes. *Journal of Geophysical Research* 95, 1837–1851.
- Sirois, A., Bottenheim, J.W., 1995. Use of backward trajectories to interpret the 5-year record of PAN and O<sub>3</sub> ambient air concentrations at Kejimikujik National Park. *Nova Scotia Journal of Geophysical Research* 100, 2867–2881.
- Staehelin, J., Thudium, J., Buehler, R., Volz-Thomas, A., Graber, W., 1994. Trends in surface ozone concentrations at Arosa (Switzerland). *Atmospheric Environment* 28, 75–87.
- Stohl, A., Kromp-Kolb, H., 1994. Origin of ozone in Vienna and surroundings. *Atmospheric Environment* 28, 1255–1266.
- Stohl, A., Spichtinger-Rakowsky, N., Bonasoni, P., Feldmann, H., Memmesheimer, M., Scheel, H.E., Trickl, T., Hübener, S., 2000. The influence of stratospheric intrusions on alpine ozone concentrations. *Atmospheric Environment* (special VOTALP section), submitted for publication.
- Stohl, A., Wotawa, G., 1995. A method for computing single trajectories representing boundary-layer transport. *Atmospheric Environment* 29, 3235–3238.
- Stohl, A., 1996. Trajectory statistics – a new method to establish source-receptor relationships of air pollutants and its application to the transport of particulate sulfate in Europe. *Atmospheric Environment* 30, 579–587.
- Stohl, A., 1998. Computation, accuracy and applications of trajectories – a review and bibliography. *Atmospheric Environment* 32, 947–966.
- Stohl, A., Wotawa, G., Seibert, P., Kromp-Kolb, H., 1995. Interpolation errors in wind fields as a function of spatial and temporal resolution and their impact on different types of kinematic trajectories. *Journal of Applied Meteorology* 34, 2149–2165.
- Tilmes, S., Zimmermann, J., 1998. Investigation on the spatial scales of the variability in measured near-ground ozone mixing ratios. *Geophysical Research Letters* 25, 3827–3830.
- Tscherwenka, W., Seibert, P., Kasper, A., Puxbaum, H., 1998. On-line measurements of sulfur dioxide at the 3 km level over central Europe (Sonnblick observatory, Austria) and statistical trajectory source analysis. *Atmospheric Environment* 32, 3941–3952.
- Vergeiner, I., Dreiseitl, E., 1987. Valley winds and slope winds – observations and elementary thoughts. *Meteorology and Atmospheric Physics* 36, 264–286.
- Virkkula, A., Maekinen, M., Hillamo, R.E., Stohl, A., 1995. Atmospheric aerosol in the Finnish arctic: particle number concentrations, chemical characteristics, and source analysis. *Water, Air and Soil Pollution* 85, 1997–2002.
- Virkkula, A., Hillamo, R.E., Kerminen, V.-M., Stohl, A., 1998. The influence of Kola Peninsula, continental European and marine sources on the number concentrations and scattering coefficients of the atmospheric aerosol in Finnish Lapland. *Boreal Environmental Research* 2, 317–336.
- Wege, K., Vandersee, W., 1991. Ozonbeobachtungen am Nordrand der Alpen. *Meteorologische Rundschau* 44, 138–146.
- Wotawa, G., 1997. Analyse und Modellierung von Ozon und anderen Luftschadstoffen in Ostösterreich. Doctoral Thesis, University of Vienna, Faculty for Natural Sciences, Institute of Meteorology and Geophysics, Austria.
- Wotawa, G., Stohl, A., Neining, B., 1998. The urban plume of Vienna: comparisons between aircraft measurements and photochemical model results. *Atmospheric Environment* 32, 2479–2489.
- Wotawa, G., Kröger, H., 2000. Testing the ability of trajectory statistics to reproduce emission inventories of air pollutants in cases of negligible measurement and transport errors. *Atmospheric Environment* 33, 3037–3043.
- Wotawa, G., Kromp-Kolb, H., 2000. The European Union research project VOTALP – general objectives and main results. *Atmospheric Environment* (special VOTALP section) submitted for publication.